ORIGINAL ARTICLE

Geo-statistical assessment of meteorological drought in the context of climate change: case of the Macta basin (Northwest of Algeria)

Sabri Berhail[1] · Mahmoud Tourki[1] · Imane Merrouche[1] · Hayat Bendekiche[1]

Abstract

Northwestern Algeria experiences a high number of spatial and temporal variations in precipitation. This phenomenon predominantly alters the duration as well as the frequency of drought in this region. The objective of this study is to detail the geographical variations in terms of drought intensity, duration, magnitude and frequency in the Macta basin using time series of rainfall data for 42 years (1970–2011) from 42 rainfall stations. The methodology employed lies in analyzing the spatial and temporal variations of rainfall along with the computation of the standardized precipitation index (SPI) to assess the spatial–temporal variations of meteorological drought over different time scales. The Sen's slope test estimator, Mann–Kendall (MK) test, and the recently developed Innovative Trend Analysis (ITA) method were used for the purpose of evaluating the precipitation trend. The application of the above-mentioned methods has shown a very notable increasing trend during autumn and a decreasing trend during spring precipitation. In this scenario, the annual, winter, and summer precipitation time series experienced a mixed (increasing as well as decreasing) trend. The magnitude of the highest increasing (decreasing) precipitation trend was found at 2.20 mm/season (− 2.55 mm/season) during autumn (spring) season. The annual precipitation trend was in the range of − 4.93 mm/year and 5.29 mm/year. A decreasing trend was observed from both MK and ITA tests in the northern part of the Mediterranean Sea, near the coastal region in Macta basin, whereas the increasing trend was observed in the south. In drought analysis, the long-term frequency drought showed that both northern and western regions faced drought conditions most of the time in comparison with southern and eastern parts of the study area. This infers that the northern and western parts lack long-term water resources. Further, the northern part of the basin usually experiences severe drought conditions when compared to other parts. Drought duration varies from 9 to 37 months with an average of 20 months. Thus, this area is cited to be highly sensitive and prone to droughts compared to other parts of the basin. These findings would be very useful in applying drought adaptation policies by water resource managers in the Macta basin.

Keywords Climate change · Drought · Spatial–temporal distribution · Standardized precipitation index (SPI) · Macta basin

Introduction

There are two major elements taken into account when studying climate change consequences. First, global models, the foremost tool in realizing this phenomenon at a global scale (Hamlet and Lettenmaier 2000; Wei and Watkins 2011; Raghavan et al. 2013), and second, station information, which is better suited for local-scale analysis. In the last few decades, rainfall changes have received much attention particularly in some areas, such as western China (Zhang et al. 2014; Chang et al. 2016) and Mediterranean basin (Caloiero et al. 2019). These regions are primarily viewed as major hotspots for climate change due to extreme drying and strong warming. The Mediterranean basin is cornered by extreme climate changes due to the interactions that occur between mid-latitude and tropical processes. Being located in a major transition zone, this basin faces the wrath of arid climate of North Africa. While at the same time, it also undergoes the rainy climate of central Europe too (IPCC 2013). Therefore, within the context of climate change, numerous studies, related to rainfall trends, have been conducted in this area.

Longobardi and Villani (2010) applied a trend tests on rainfall time series from 211 stations over a period of 81 years (1918–1999) in the Campania region in Southern Italy. The study results concluded that the trends, i.e.,

✉ Sabri Berhail
berhail_sabri@yahoo.fr

[1] Department of Technical Sciences, Abdelhafid Boussouf University Center, P.O. Box 26, 43000 Mila, Algeria

annual as well as season scale were negative ones excluding the summer period. Da Silva et al. (2015) conducted a study with data collected for 40 years from the Cobres River basin, Southern Portugal. The authors used Mann–Kendall and Sen's methods to analyze the trend in precipitation. They concluded that there was a decrease found in the rainfall amount recorded annually. These kinds of studies are conducted elsewhere, excluding the Mediterranean region too. For instance, Batisani and Yarnal (2010) applied the Mann–Kendall (MK) test to detect the variations in rainfall for both annual and monthly time periods in semi-arid areas of Botswana. The study results inferred a decreasing trend both annually as well as monthly with July as the only exception during when the increasing trend was observed. The study conducted by Gocic and Trajkovic (2013) deployed non-parametric Mann–Kendall and Sen's method to detect annual as well as seasonal trends for seven different meteorological variables during the period, 1980–2010 in Serbia. The study confirmed the absence of a significant trend in rainfall. Duhan and Pandey (2013) conducted a study in which they deployed Sen's slope estimator test and Mann–Kendall (MK) test for rainfall time series in Madhya Pradesh, India. They took data for 102 years (1901–2002) and the results showed a decreasing pattern annually. The seasonal analysis exhibited a notable increase in the trend during summer, while the decreasing trend was observed during monsoon timings. Gedefaw et al. (2018) conducted a study upon annual as well as seasonal rainfall variability deploying the ITAM method (Innovative Trend Analysis Method). The study compared the results from the MK test (Mann–Kendall) and Sen's slope estimator test at five specific stations located in Ethiopia in the Amhara region. The results inferred that there was an increase found in the rainfall trend at a few stations, while other stations experienced a decrease. On the basis of monthly scale and seasonal scale, there was an increasing trend observed in the months spanning May and September. In case of other months, a decreasing trend was observed. In another research, Derdous et al. (2020) used Mann–Kendall test, Sen's method, and Pettitt test for identification of trends and change points in the annual rainfall over the period from 1936 to 2008 in the Cheliff Basin (Northwestern Algeria). The results showed that the annual rainfall had a statistically significant downward trend in the whole basin. Further, according to the Pettitt test, this decrease scenario happened during the decade 1970–1980 at the majority of the studied rainfall stations. The tests of stationarity were less used when it comes to rainfall time series in comparison with other two statistical tests, such as compared homogeneity and trend analysis (Machiwal and Jha 2008; Khalil et al. 2017).

According to researchers, precipitation remains a crucial climatic variable and directly influences the patterns of the flood (Kim et al. 2016; Azam et al. 2017) and drought (Maeng et al. 2017; Azam et al. 2018; Nair and Mirajkar 2020). Due to recent climate change patterns observed across the globe, there is a significant amount of attention aid upon quantitative drought prediction. In the recent years, there are different indices proposed for use in drought prediction and more than dozens of indices were revised by researchers in the past (Keyantash and Dracup 2002; Mishra and Singh 2010; Zargar et al. 2011; Kebede et al. 2020). But the drought indices which consider rainfall data as it is basis, are simple to execute and produce excellent performance (Oladipo 1985). When it comes to drought assessment, there are few indices that generally leverage rainfall data, such as standardized precipitation index (SPI) (Mckee et al. 1993), while the latter is often utilized across the globe (Hosseinizadeh et al. 2015; Ghosh 2019; Gyamfi et al. 2019; Sobhani and Zengir 2020; Pathak and Dodamani 2020; Rousta et al. 2020). Mekonen et al. (2020) suggested that SPI is more suitable for monitoring droughts in East Africa because it is easily adapted to the local climate and it produces spatially consistent results. SPI is deemed to be the standard drought monitoring index proposed by World Meteorological Organization (WMO) (Hayes et al. 2011). The Indian Meteorological Department (IMD) also uses it as one of the two indices while the other being, 'Aridity Anomaly Index'. Likewise, the SPI is a very suitable index to study the geospatial and temporal variation of drought with spatially invariable results for historic time series analysis (Masih et al. 2014; Ghosh 2019).

The analysis of the spatio-temporal drought features in northern Algeria including spatial extent, severity and duration is important for understanding the nature of drought and evaluating the region's vulnerability as well as for developing models to investigate different drought properties. In recent decades, many studies have been conducted to investigate drought trends and their relation to other variables in Algeria (e.g. Touchan et al. 2011; Mellak and Souag-Gamane 2020; Derdous et al. 2020; Achour et al. 2020). To the best of our knowledge, none of them have applied the SPI model to characterize the geographical variations of drought risk as a function of intensity, duration, magnitude and frequency.

The current research paper has the following primary objectives: (i) to identify the spatial and temporal trends in annual and seasonal rainfall in the Macta basin, Northwest Algeria with the help of Mann–Kendall (MK) test, Sen's slope test estimator and the recently developed Innovative Trend Analysis (ITA) method; (ii) to detail the geographical variations of drought intensity, duration, magnitude and frequency for two time scales, such as 6-month (SPI-6) and 12-month (SPI-12).

Study area and data

Figure 1 shows the Macta Basin (14,389 km^2) in north-western Algeria which is the largest basin in the country, in terms of surface area. There are two main rivers that drain it, such as Mekerra and El Hamman. While the former is in its uppermost part and the latter is located at western and eastern sectors, respectively. This study area is generally characterized by mountain-based landscape. To be precise, the basin has boundaries, such as carbonatic Tessala Mountain in the north, Maalif high plateau in the south, Telagh plateau in the west, and Saida Mountains in the east. With regard to sand types, wide and shallow alluvial plain soil, which is primarily of sandy-clayey type, can be found in addition to marly-clayey deposits (Perrodon 1957). There is a difference, in that mountainous landscape and the coastal plain are found with Aeolian dunes.

El Mahi et al. (2012) noted that the study area is surrounded by desert region and shrub in the southwestern sector, whereas the Middle-Western region has a forest area. Arable land is present in abundant quantities in the eastern region. There is a pattern of high spatial and temporal variabilities of annual precipitation observed in Macta basin (Meddi et al. 2010a, b). The basin's annual precipitation lies in the range of 280 mm in the south to 600 mm in the north (Laborde 1993). The northern region

is characterized by typical warm Mediterranean whereas it prevails with a dry season from April to August–September and a wet season from September to March. The southernmost region of the Macta basin is characterized by cold semiarid climate.

In the current study, a number of studies were reviewed and exploited to acquire sufficient knowledge. Further, a number of visits were paid to ONM (National Office of Meteorology) and ANRH (National Agency of Hydraulic Resources) along with repeated field surveys for the study. For the period 1970–2011, monthly rainfall data were collected from 42 meteorological stations in the Macta basin. Figure 1 shows the spatial distributions of the 42 stations studied and Table 1 lists their characteristics.

Methodology

Trend analysis

Innovative Trend Analysis (ITA) method

Sen (2012) proposed the ITA method which segregates any kind of hydro-meteorological time series into two halves of equal size followed by its sorting into sub-series in ascending order. The horizontal axis has the first half series (x_i) while the vertical axis has the second half series
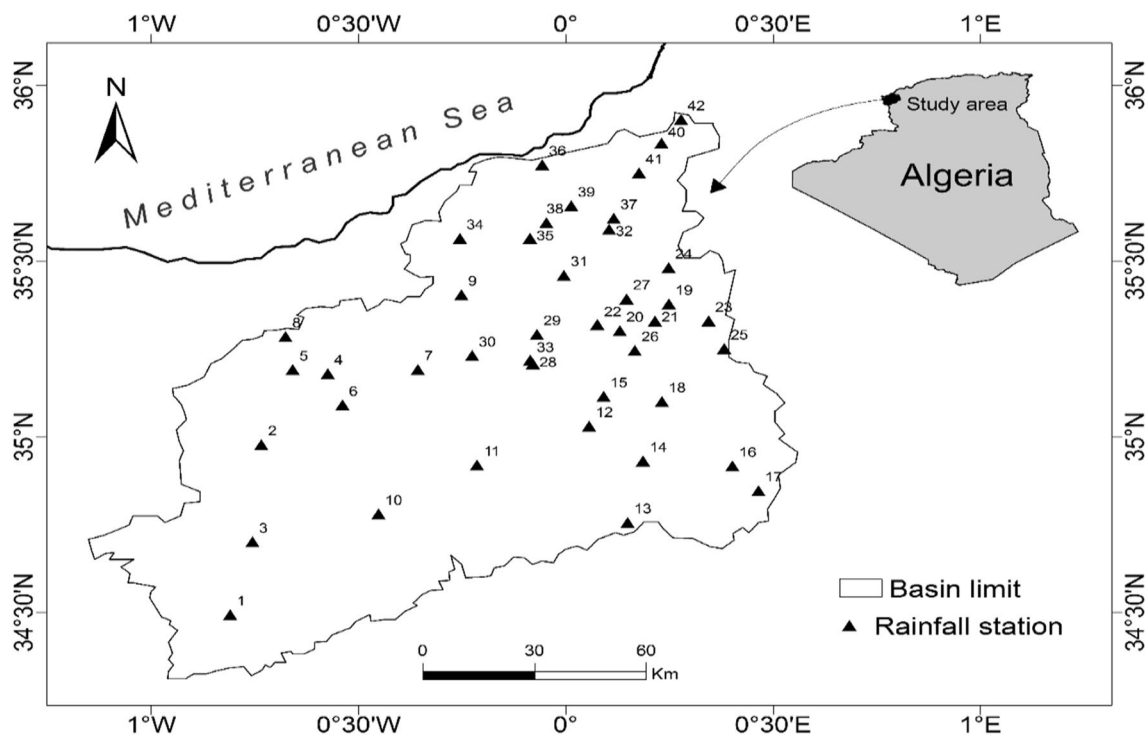

Fig 1 Geographical situation and rainfall station of the Macta basin

Table 1 A summary of the information on rainfall stations used in the study (period: 1970–2011)

No	Station name	Station code	Longitude (°)	Latitude (°)	Altitude (m)
1	RAS EL MA	110102	−0.80933	34.49474	1097
2	SID ALI BEN YOUB	110201	−0.73404	34.97824	635
3	EL HACAIBA	110203	−0.75556	34.70201	950
4	SARNO Bge	110304	−0.57406	35.18035	425
5	SIDI BEL ABBES	110305	−0.65858	35.19152	485
6	HASSI DAHO	110309	−0.53858	35.09111	650
7	MOSTEFA BEN BRAHIM	110312	−0.35696	35.19200	590
8	AIN TRID	110314	−0.67574	35.28576	530
9	CHEURFAS BGE	110402	−0.25162	35.40439	230
10	MERINE	110501	−0.45176	34.78133	970
11	DAOUD YOUB	110802	−0.21412	34.92048	660
12	MEFTAH SIDI BOUBEKEUR	111102	0.05598	35.03100	530
13	AIN EL HADJAR	111103	0.14913	34.75705	1025
14	HAMMAM RABI	111112	0.18628	34.93192	710
15	OUED TARIA	111201	0.09105	35.11565	501
16	AIN TIFRIT	111204	0.40185	34.91781	970
17	TAMESNA	111210	0.46458	34.84732	1105
18	BENIANE	111217	0.23145	35.10107	630
19	MAOUSSA	111401	0.24820	35.37831	494
20	FROHA	111402	0.13004	35.30213	467
21	MATEMORE	111405	0.21502	35.32982	482
22	TIZI	111413	0.07612	35.32007	453
23	SIDI KADA	111414	0.34432	35.33020	549
24	AIN FARES	111417	0.24778	35.48157	806
25	NESMOTH MF	111418	0.38181	35.25157	930
26	GHRISS	111424	0.16650	35.24627	498
27	MASCARA	111429	0.14642	35.39286	550
28	SAHOUET OUIZERT	111502	−0.07953	35.20784	361
29	BOU HANIFIA BGE	111503	−0.06980	35.29195	306
30	SFISSEF	111508	−0.22602	35.23183	545
31	HACINE	111509	−0.00453	35.45988	145
32	MOHAMMADIA GRHA	111511	0.10420	35.59037	50
33	TROIS RIVIERES	111516	−0.08594	35.21851	315
34	OGGAZ	111604	−0.25537	35.56487	73
35	BOU HENNI	111605	−0.08649	35.56532	26
36	FORNEKA	111606	−0.05675	35.77438	78
37	SAMOURIA	111607	0.11531	35.62218	48
38	MOCTA DOUZ	111610	−0.04662	35.60955	18
39	FERME BLANCHE	111611	0.01306	35.65736	20
40	BLED TAOURIA	111612	0.23074	35.83568	118
41	MARAIS DE SIRAT	111616	0.17641	35.75066	30
42	FERME ASSORAIN	111617	0.27798	35.90293	222

(y_i) in the Cartesian coordinate system. The diagram is divided into two equal triangles by a bisector line at 1:1 (45). The increasing trend is denoted by the upper triangle while a decreasing trend is indicated by the lower one. To determine the trend, the ITA-drawn straight-line trend slope (s) is calculated based on the equation given below.

$$s = \frac{2(\bar{y}_2 - \bar{y}_1)}{n}, \tag{1}$$

in which $\bar{y}_1$ and $\bar{y}_2$ denote the arithmetic averages for first as well as second halves of the dependent variable, whereas the number of data is denoted by n. Further, the

arithmetic averages of the two halves are shown as 'centroid point' that falls on the data line.

The innovative templates enable the researcher to understand the interpretation with linguistic facility for the trend i.e., 'low', 'medium', and 'high' as shown in Fig. 2. Then, it is possible to either increase or decrease the trend interpretations based on the position of data scatter points in each portion and their positions above or below the 1:1 no-trend line, in case when the horizontal axis' biggest data value range is divided into three equal portions. Further, one portion can be compared with another portion and vice versa too (Dabanli et al. 2016). Ahmad et al. (2018) confirmed that the ITA plot could identify the sub-trend of rainfall time series over the upper Indus River basin. Likewise, Serencam (2019) also proved that the ITA method is more dependable in detecting trends in meteorological time series.

According to Sen (2014), if the scatter points are further to 1:1 line, then the trend exists severely with higher slope values. Considering these points into account, different signs were used to represent the necessary interpretations in this study. Among these, o implies no-significant trend, $+ (-)$ exhibits significant increasing (decreasing) trend, $+ + (- -)$ denotes more significantly increasing (decreasing) trend than the previous portion, and finally $+ + + (- - -)$ implies very significant increasing (decreasing) trend than the two previous portions. These templates show excellent use in variability feature interpretations as explained in detail by Sen (2015). As per Fig. 2, the variability has a relationship with standard deviation centroid position in novel trend templates. One can infer that there exists an increasing (decreasing) variability within the record series, if the standard deviation centroid is below (above) the no-trend line (1:1 line).
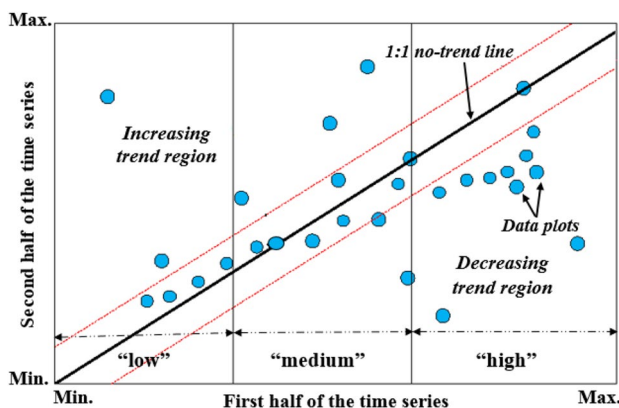
Mann–Kendall trend test

Being a rank-based nonparametric test, MK test gained popularity among researchers in the recent years since it is applied to identify the trends in rainfall data (Mann 1945; Kendall 1975; Krishnakumar et al. 2009; Shifteh Somee et al. 2012; Kumar et al. 2016; Geremew et al. 2020). The following formula is used to conduct the Mann–Kendall test statistic S.

$$S = \sum_{i=1}^{n-1} \sum_{j=i+1}^{n} \text{sign}(x_i - x_j). \tag{2}$$

In the above equation, n denotes the dataset length, while the two generic sequential data values are denoted as x_i and x_j.

The function sign $(x_i - x_j)$ assumes the following values:

$$\text{sign}(x_i - x_j) = \begin{cases} 1 & \text{if } (x_i - x_j) > 0 \\ 0 & \text{if } (x_i - x_j) = 0 \\ -1 & \text{if } (x_i - x_j) < 0 \end{cases}. \tag{3}$$

In the above equation, when S is high and positive, it establishes the fact that there is an increasing trend present. While an extremely low negative value denotes the trend is decreasing. The variance of S, for the situation where there may be ties (that is, equal values) in the x values is given by:

$$\text{Var}(S) = \frac{n(n-1)(2n+5) - \sum_{i-1}^{m} t_i(t_i - 1)(2t_i + 5)}{18}, \tag{4}$$

where n denotes the number of data points following by t_i denoting the number of ties for i value and m represents the number of tied values. Both the Eqs. (2) and (4) are utilized to determine the test statistic Z based on the equation given below:

$$Z_{\text{MK}} = \begin{cases} \frac{S-1}{\sqrt{\text{Var}(S)}} & \text{if } S > 0 \\ 0 & \text{if } S = 0 \\ \frac{S+1}{\sqrt{\text{Var}(S)}} & \text{if } S < 0 \end{cases}. \tag{5}$$

The trend direction is denoted by the sign, Z. The increasing trend can be mentioned as significant, if the positive Z value is higher than 1.96 (on the basis of normal probability tables) at the 0.05 significance level. In case of a negative Z value less than -1.96, the trend is inferred to be decreasing in a significant manner.

Sen's slope estimator

Sen (Sen 1968; Theil 1950) proposed this approach to determine the magnitude of the trend in rainfall time series and is estimated as follows:

Fig 2 An example of the innovative trend analysis (ITA) method shows increasing and decreasing trend regions

$$\beta = \text{median}\left(\frac{x_j - x_k}{j - k}\right), \tag{6}$$

where x_j and x_k denote the data values at time j and k $(j > k)$, respectively. A positive value of β denotes that the trend is increasing, while the trend is said to be decreasing if the value is negative in time series data (Xu et al. 2010).

Percentage change in magnitude

The change percentage is generally calculated by approximating it, with linear trend. Yue and Hashino (2003) defined this method in which the change percentage is equal to the value achieved through multiplication of period length and median slope, divided by the corresponding mean. This value is expressed in terms of percentage.

$$\text{Percentage change (\%)} = \frac{\beta * \text{lenght year}}{\text{mean}} * 100. \tag{7}$$

Drought quantification

Standardized precipitation index (SPI)

McKee et al. (1993) developed Standardized precipitation index (SPI) on the basis of probability distribution of precipitation to monitor drought at multiple time scales. In simple use, SPI is calculated by taking the difference of the precipitation, X_i from the mean, $\overline{X}$ for a particular time step, and then dividing it by the standard deviation, σ (Sonmez et al. 2005).

$$\text{SPI} = \frac{X_i - \overline{X}}{\sigma}. \tag{8}$$

The severity of drought events is generally classified as moderate, severe and extreme based on SPI values, i.e., 1.00 to − 1.49, − 1.50 to − 1.99, and ≤ − 2.00, respectively (WMO 2012). It is possible to calculate the SPI for various time scales, such as 1 month, 48 months or even longer. These time scales exhibit the influence of drought on the accessibility of various water resources. However Ji and Peters (2003), suggested that SPI on a short timescale like 3 or 6 months is appropriate for detecting drought events that affect agricultural practices, while the longer timescale, such as 12 or 24 months, is more suitable for water resources management purposes (Potop et al. 2014). In this study, SPI was computed for time scales of 6 months (SPI-6) and 12 months (SPI-12) to explore the drought variation at inter-seasonal and inter-annual time scales.

The 6-month SPI compares the precipitation for that period with the same 6-month period over the historical record. For example, a 6-month SPI at the end of September compares the precipitation total for the April–September period with all the past totals for that same period. The 6-month SPI indicates medium-term trends in precipitation and is still considered to be more sensitive to conditions at this scale than the Palmer Index. A 6-month SPI can be very effective showing the precipitation over distinct seasons. Information from a 6-month SPI may also begin to be associated with anomalous stream flows and reservoir levels.

A 12-month SPI is a comparison of the precipitation for 12 consecutive months with that recorded in the same 12 consecutive months in all previous years of available data. The SPI at these timescales reflects long-term precipitation patterns. Because these time scales are the cumulative result of shorter periods that may be above or below normal, the longer SPIs tend toward zero unless a specific trend is taking place.

Drought risk evaluation parameters

The already known concepts related to the drought process are the drought duration, drought magnitude and drought intensity. Also, the relative frequency is used to assess the percentage of the number of drought locations in the total study area (%) for different drought categories. Therefore, it indicates the percentage of area affected by drought (Li et al. 2012; Gidey et al. 2018). These concepts are defined as follows:

Drought duration (D) is the length of the period during when the SPI remains continuously negative (Spinoni et al. 2014). Starting from − 1.0 or less, the event ends when the SPI values turn into positive.

Drought magnitude (DM) and mean intensity (MI) correspond to the cumulative water-deficit over a drought period (Thompson 1999) and the average of this cumulative water-deficit over the drought period is mean intensity. Thus, DM is the absolute value of the sum of all SPI values during a drought event (Eq. 9) and MI of a drought event refers to magnitude divided by duration (Eq. 10).

$$\text{DM} = \sum_{j=1}^{n} \text{SPI}_{ij}, \tag{9}$$

$$\text{MI} = \frac{D_M}{D}, \tag{10}$$

where DM denotes the drought magnitude, j is the first month with negative SPI values, n is the last month of dry period.

Furthermore, the relative frequency (RF) is attained by dividing the number of months with drought evens (Negative SPI) by number of total months. The relative frequencies were used to assess the drought liability during a

study period (Wang et al. 2014) or return period as follows (Eq. 11):

$$\text{RF} = \frac{Nj}{j.n} * 100, \tag{11}$$

where Nj denotes the number of months with droughts for time scale j in the n-year set; j is time scale (6 and 12 months), n denotes the number of years in the data set.

Results and discussion

Temporal trend analysis using the ITA method

The results of the application of the ITA method for a total of 42 meteorology stations scattered at various regions of the Macta Basin are summarized in Table 2. It shows the trend and slope calculation results, which includes half series (1970–1990 and 1991–2011) arithmetic averages as well as standard deviations values coupled with trend slope values. Figure 3 infers that there exists four different types of innovative trend templates based on the increasing and decreasing trend components, and neutral case in each group of 'low'-, 'medium'-, and 'high'-rainfall values (Brunetti et al. 2004; Alashan 2018).

The innovative trend template shows that all the data scatter points, according to Fig. 3a, lie above the 1:1 straight line. This infers that there exists an increasing trend leaving behind the 'low-, medium- and high'-rainfall values. The arithmetic average as well as standard deviation centroids was found to be above the no-trend line in these graphs. Thus, it infers the increasing trend on average and standard deviation. In case of high-rainfall values, it is apparent that the trends gain more effectiveness since the high-rainfall points are distanced away from 1:1 straight line in comparison with 'low- and medium'-rainfall values. This case is valid for two stations, such as 110102 and 110802, located at the Eastern medium part of Macta basin, where an effective continental climate is present.

The Macta basin stations, close to half in number, exhibited a decreasing trend leaving aside the groups present in the graphs of Fig. 3b. This might be due to the fact that all the scatter points fall under no-trend line of 1:1 straight line. One can say that every station observed the decreasing trend to be the highest, when the rainfall value is high as it is the furthest point from 1:1 straight line. Two stations, i.e., 110314 and 110312, located at the northern and eastern parts of the basin showcased this trend since they are close to Mediterranean Sea coastal area. From the previous studies, it is understood that the Mediterranean region undergoes climate change effect due to increase in temperature and decreased pattern of precipitation trends

(IPCC 2013). Achite et al. (2017) also found an increase in temperature between 1970 and 2000s resulted in response to climate change, and precipitation moved forward during the late warm season in which the Macta basin experienced an increase in variability at the inter-annual scale.

The stations, such as 110501 and 111102, shown in Fig. 3c exhibited decreasing or no-significant trends in case of 'low and medium' precipitation ranges. However, in case of 'high'-rainfall values, the increasing trend was observed. This outcome may be the forerunner for the increased frequency of flood in the future. At the end, Fig. 3d shows the innovative trend templates with station numbers, 111112 and 111402 with decreasing trend during the 'high'-rainfall range. There were different trends observed in case of 'low and medium' groups.

Figure 4 shows the interpretations for increasing and decreasing trend cases indicated by ∆ and ∇ signs, respectively. Once the increasing (+) and decreasing (−) trend slope signs were conveniently inserted in the Table 2, there is a clear picture available about the prevailing scenarios, i.e., the sub-region of decreasing trends were found near the northern part proximity to Mediterranean Sea coastal area in the Macta basin. On the contrary, the trends were increasing at the southern end. This might be attributed to climate change for which we can predict its effects at higher elevation areas. In meteorological terms, the northern part of the Macta basin is subjective to Mediterranean climate. There is a continental trend continues in the south which relatively infers the marked aridity, cold winters, and particularly hot summers (Meddi et al. 2009). These results are in accordance with those obtained by Elouissi et al. (2017) by showing that climate tends to shift from south to north in the Macta basin. These changes have implications on hydrological extremes like droughts and floods. They can also affect growing seasons and crop yields (Meddi et al. 2009; Sultan et al. 2014).

Trend analysis using Mann–Kendall test

Annual trends of precipitation

The direction (Z value) and percentage changes (change %) for annual and seasonal rainfall were determined over a period of 42 years (1970–2011) in the Macta Basin, as shown in Table 3. The increasing and decreasing trends are denoted by positive and negative Z values, respectively. In Fig. 5, the spatial pattern is shown for annual as well as seasonal precipitation trends for all the 42 rainfall stations considered in this study. The annual precipitation time-series analysis using the MK test inferred that less than 50% of the stations had a positive trend, i.e., 17 of 42 stations or 40%, whereas 25 stations, i.e., 60% experienced a negative trend as shown in Fig. 5a. A total of 7 stations identified with a

Table 2 Innovative trend analyses parameters

No	Station code	1970–1990 Mean (mm)	1991–2011 Std. D. (mm)	Trend Mean (mm)	Interpretation Std. D. (mm)	Slope (–)	Low	Medium	High
1	110102	12.96	16.29	20.08	23.38	0.0282	+	+ +	+ +
2	110201	27.78	30.72	30.95	34.16	0.0125	o	+	+ +
3	110203	24.87	27.83	26.05	27.97	0.0046	o	−	−
4	110304	32.54	38.02	27.16	29.41	− 0.0213	−	− −	− −
5	110305	27.88	31.87	26.91	28.32	− 0.0039	o	−	−
6	110309	28.04	32.34	26.6	30.87	− 0.0057	o	−	−
7	110312	29.73	36.39	24.68	28.5	− 0.0224	−	− −	− − −
8	110314	38.11	43.6	29.28	31.85	− 0.0351	−	− −	− −
9	110402	27.16	33.47	25.78	28.91	− 0.0054	o	o	+
10	110501	25.38	26.88	28.16	28.4	0.0111	o	−	+
11	110802	16.35	18.68	22.04	23.17	0.0226	+	+ +	+ +
12	111102	22.36	28.03	24.88	27.15	0.0099	o	o	+
13	111103	26.65	31.42	30.52	31.08	0.0153	o	o	−
14	111112	19.78	24.53	25.41	25.77	0.0223	+	+	−
15	111201	23.62	30.13	23.18	23.43	− 0.0017	o	o	+
16	111204	31.69	33.59	28.06	29.01	− 0.0144	o	−	+
17	111210	26.37	27.59	27.9	32.16	0.0061	o	o	+
18	111217	21.68	27.64	30.39	33.7	0.0345	+	+	+ +
19	111401	24.93	30.01	25.18	26.89	0.0009	o	−	−
20	111402	22.8	28.35	24.94	25.95	0.0085	+	o	−
21	111405	26.6	27.92	22.28	23.19	− 0.0171	o	−	− −
22	111413	28.79	32.18	28.42	29.67	− 0.0015	o	o	−
23	111414	29.17	29.75	30.92	32.51	0.0069	o	−	−
24	111417	28.55	33.65	38.42	41.14	0.0391	+	+ +	+ +
25	111418	38.51	42.88	39.59	43.5	0.0042	o	o	+
26	111424	27.85	33.35	22.07	23.05	− 0.0229	o	−	− −
27	111429	26.27	31.32	30.01	32.44	0.0148	o	+	+
28	111502	20.83	23.28	20.84	21.77	0.0001	o	−	−
29	111503	21.49	27.05	20.03	22.31	− 0.0057	−	− −	− − −
30	11108	24.64	28.27	21.13	22.74	− 0.0139	−	− −	− − −
31	111509	27.24	34.48	25.49	23.34	− 0.0069	o	−	− −
32	111511	27.26	32.98	24.28	27.28	− 0.0118	−	− −	− − −
33	111516	19.33	25.4	18.71	20.08	− 0.0025	o	−	− −
34	111604	22.05	27.44	20.93	25.54	− 0.0044	o	−	− −
35	111605	21.49	27.05	20.03	22.31	− 0.0057	−	−	− − −
36	111606	23.4	30.68	20.33	23.62	− 0.0121	−	− −	− − −
37	111607	24.65	30.31	21.12	23.94	− 0.0141	o	−	− −
38	111610	18.43	26.36	28.25	32.59	0.0389	+	+ +	+ +
39	111611	25.72	30.46	24.13	25.48	− 0.0063	o	−	− −
40	111612	26.64	35.08	26.5	30.32	− 0.0005	o	−	− −
41	111616	24.77	32.33	22.97	26.91	− 0.0071	o	−	− −
42	111617	28.58	35.01	25.08	29.04	− 0.0139	o	−	− −

significant trend with a 95% confidence level when using Z value level (four stations had a positive trend, whereas three stations exhibited a negative trend). The southern part of the basin expressed mostly significant positive trends. While the east-central region exhibited significant negative trends.

Figure 6a showcases the trend magnitude of annual precipitation (mm/year). There is a gradual decline observed in the slope of the trend magnitudes from southwest to northeast direction. This differed from − 4.93 mm per year to 5.29 mm per year from 1970 to 2011.

The most negative trend is measured at Ain Trid (− 4.93 mm per year), followed by (− 2.85 mm per year) at Sfissef and Matemore (− 2.81 mm per year). A dramatic and widespread decrease in annual precipitation is observed, accounting for 16% of the mean annual precipitation in the study period of 42 years. These results are in line with the conclusions of Meddi et al. (2010a, b) and Berhail (2019) who found a reduction of atleast 20% of total annual rainfall at 12 rainfall stations in Macta and Tafna basins.

Seasonal trends of precipitation

Autumn There was an increasing trend found in the autumn precipitation series across the study area for major stations i.e., 40 out of 42 (95%). While the remaining two stations reported a decreasing trend (Fig. 5b). A total of 10 stations yielded significance (95% confidence level) with positive trend and no significance achieved in case of a negative trend (Table 3). As can be seen in Fig. 5b, autumn season exhibits increasing precipitation trends. Significant positive trends are mostly found in the southern part of the basin. The magnitude of the trend differed in the range of − 0.29 and 2.20 mm/season per year (Fig. 6b). A general conclusion is that there is an increase observed in the precipitation value for autumn season over 42 years. These results are in alignment with other researchers (Benzater et al. 2019; Bougara et al. 2020) who conducted their studies in northwest Algeria. According to the study carried out by (Dünkeloh et al. 2003; Tramblay et al. 2012), the positive trend of rainfall in autumn can be best understood through positive anomalies in the rainfall amount recorded in North African regions. This increment might be attributed to the impact created by a negative trend of the North Atlantic Oscillation (NAO) index. This negative phase has a correlation with a storm track that is denoted in the pressure associated with lower Azores height, compared to the normal value. In parallel, there exists the formation of Icelandic Low. The formation of the depression traffic mode results in drawing it further south, creating an impact upon Mediterranean regions of the south shore resulting in wetting (Nouaceur and Murărescu 2016). This is detailed through an increment in the rainfall amount. This further corresponds with extreme temperature that has a strong connection with the NAO index, in which there exists an association between negative period and extremely high temperatures (Donat et al. 2014; Báez et al. 2019) which affect the Western African in the Mediterranean region.

There is a strong NAO index present that affects the Southwestern Mediterranean region, when compared to El Nino Southern Oscillation ENSO index. This is because the latter is highly significant at the eastern parts of the Mediterranean region. This is an established scenario due to the proximity of the areas in which these two modes of variability function are used (Donat et al. 2014).

Winter Negative trends were observed in half of the stations i.e., 22 out of 42 stations (52%) compared to positive trends using the MK test as shown in Fig. 4c. But the results also found no-significant shift during the winter precipitation time series for the period 1970–2011. The negative trends were predominantly found in the western region of the Atlas Mountains (Fig. 5c). It can be understood from the Fig. 6c that the spatial distribution of winter precipitation trend magnitude differed in the range of − 1.36 and 2.03 mm/season per year. The winter season was reported to undergo reduction in precipitation trends during the study period of 42 years. In a previous study Benzater et al. (2019) also found similar results for the period 1970–2011 and reported that a significantly decreasing trend in the winter season in the same basin.

Spring From MK test, it was found that 33 out of 42 stations (79%) exhibited negative trends as shown in Fig. 5d. There were only two stations reported to have a significant negative trend with 95% confidence level. During spring season, the basin experienced a decrease in the unlike autumn season. The differences in the range of trend magnitude during spring precipitation were in the range of − 2.55 and 0.8 mm/season per year (Fig. 6d), inversely proportional to autumn scenario. This study findings with regards to decreasing spring trends are in alignment with the findings of Belarbi et al. (2017) in northwest Algeria. A similar decreasing trend is also reported in the Mediterranean region of Northern Morocco (Knippertz et al. 2003; Meddi et al. 2010a, b; Ghenim et al. 2010) and can be explained by a change in atmospheric circulation (Wang et al. 2010).

Summer There were contradictory precipitation trends achieved in case of summer, when compared with winter. A total of 25 (60%) stations showed positive trends while 16 (38%) stations exhibited negative trends as shown in Fig. 5e. There were only three stations observed with significant positive trends while no-significant negative trends were observed in any of the stations (Fig. 5e). There were significant positive trends achieved in the northwestern part of the basin. Mild positive slopes were reported by spatial distribution except coastal zone. Few regions in the central-western basin exhibited mild negative trend magnitude. In line with autumn, the summer precipitation trend magnitude also exhibited difference between − 0.1 and 0.57 mm/season per year (Fig. 6e). To conclude, the summer season is said to have experienced mild increasing precipitation trends over 42 years.
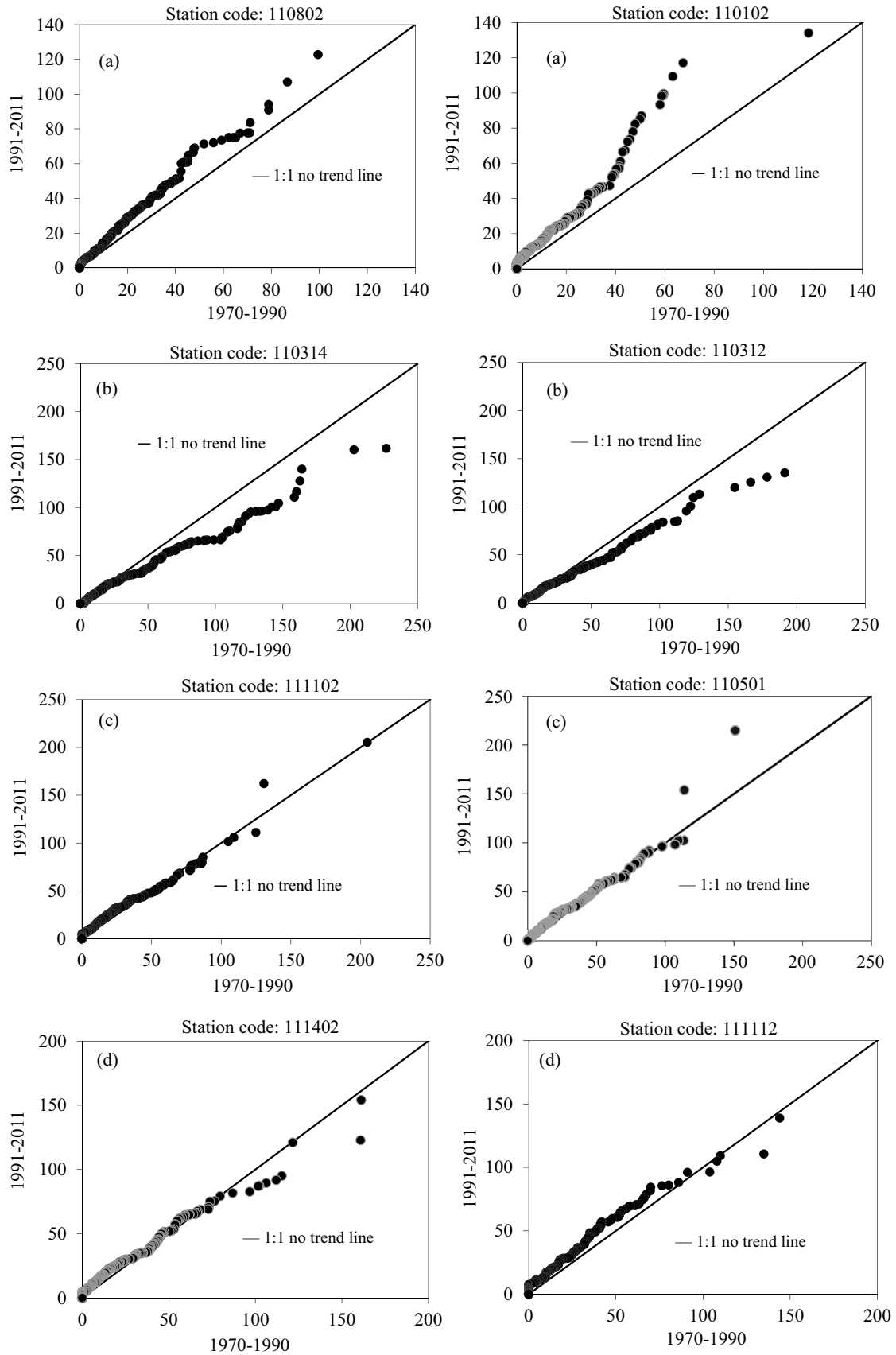
◀**Fig 3** ITA analysis method for annual rainfall at **a** Generally increasing trend, **b** generally decreasing trend, **c** increasing trend at high rainfall record values, **d** decreasing trend at high rainfall record values

Spatial and temporal assessment of the drought

As mentioned earlier, it is mandatory to have a good fit of gamma frequency distribution for the precipitation data, if one needs to calculate SPI for a specific time scale. In Table 4, a summary of drought characteristics can be found for the period 1970–2011 for all the stations in the basin on a 12-month time scale. Though the data is not shown, similar characteristics were also obtained on a 6-month scale. On the basis of 6-month SPI, various droughts were reported during 1970–2011. Of these droughts, the most significant were 1981–1982, 1983–1984 and 1996–1999. A total of 19 months from April 1983 to November 1984 was the longest duration of the drought recorded. In line with this, the drought of 1984 lasted 18 months with -3.72 peak intensity (extremely dry) and a mean intensity of -2.33 under severe classification. The SPI peak intensity (-3.72) of this time scale occurred in September 1984. The relative frequency of droughts of this time scale was approximately 14.09%. In a similar vein, Mekonen et al. (2020) reported that 1984 stands the main horrible year on the record in the northeastern highlands of Ethiopia.

Table 4 results infer that almost all the stations suffered peak intensities of less than -2 which falls under extreme classification. The noticeable stations had -3 peak intensity. The peak intensities were mostly found in the decade of 1980, especially 1983. The highest intensity ($SPI = -3.93$) occurred during the period, March 1982 at Hacine station (111509). The Ras El Ma station (110102) experienced the longest drought from April 1976 to January 1979, a period of 34 months with peak intensity, magnitude and mean intensity values being -2.94, -70.22, and -2.07, respectively. The Hammam Rabi station (111112) underwent a 33-month drought with -58.31 magnitude and -1.77 mean intensity. The drought which spanned for 12 months during 1997–1988 had a magnitude of -27.35 with -2.28 mean intensity at Ain Trid station (110314) in northwestern part. This drought heavily influenced the region when compared to the droughts that occurred earlier. As shown in Table 4, almost all the stations experienced the longest, most and intense droughts during 1980s.

The relative frequencies of Forneka station (111606), Sahouet Ouizert station (111502), Mostefa ben brahim station (110312) and Mascara station (111429) (18.65%, 18.45%, 18.06%, and 17.06%, respectively) are more significant than others. These findings are consistent with those of previous studies. Indeed, Achour et al. (2020) reported that the rise of drought events was significant only for the second half of 1970s, early 1980s and end of 1980s decade at

9- and 12-month scales in northwestern Algeria. Likewise, Khedimallah et al. (2020) analysed rainfall and hydrometric regimes over the period from 1968 to 2013 on the Cheliff basin situated in the west and the Medjerda basin in the east of Algeria. The results obtained reveal that the basins represent a marked spatial and temporal variability with a downward trend as early as the 1970s, with an increase in the frequency of dry years. Severe droughts have been recorded after 1980 in both basins with a total reduction exceeds 30%. Furthermore, Jemai et al. (2018) analysed the spatiotemporal variability of rainfall in Northern Tunisia. The results indicate a severe persistent drought occurred since the end of the 1970s. Over the Oum Er-Rbia river basin (Morocco), the rainfall trends and droughts have analysed during the period 1970–2010 by Ouatiki et al. (2019) using SPI and Mann–Kendall test. The results show a tendency towards drier conditions most occurred between the 1980s and 1990s with a deficit exceeds 50% of the seasons.

Duration, severity and intensity of drought

As mentioned earlier, the SPI characteristics computed for medium to long-term trends were utilized to develop drought maps for Macta basin following IDW methodology. This is done to interpolate the station data in GIS software.

Figure 7a shows the 6-month drought intensity map with heavy intensities in the central part compared to southwestern and northeastern regions. This map has more number of high intensity affected areas compared to its counterpart. Figure 7b shows the 12-month drought intensity map which infers that the basin's southern western and central parts underwent high intensities compared to east, and north outlets for a period of 42 years. Large areas got affected in spite of the fact that the intensity values of this time scale are high than 6-month SPI.

Figure 8a shows the 6-month SPI drought duration map from which it can be understood that southern and central parts underwent extended droughts than the northern and outlet parts of the basin. But this kind of extended durations were experienced by most parts of the region, which started decreasing from south, southeast and northwest towards the outlet. In line with the prediction, there were high number of drought durations found by 12-month SPI when compared to 6-month SPI. Figure 8b shows the drought duration map for 12-month SPI with longer durations almost spread across the whole basin region, excluding northeast and west-central parts of the basin. For the period 1970–2011, the average magnitude of the longest drought was -29 and the most intense drought was -26 on a 12-month scale (Fig. 9a, b). The mean intensity values were -2.07 and -3.21. It can be noticed that the region suffered from an extended drought while its magnitude also was found to be higher.

Fig 4 Spatial trend partition of the Macta basin
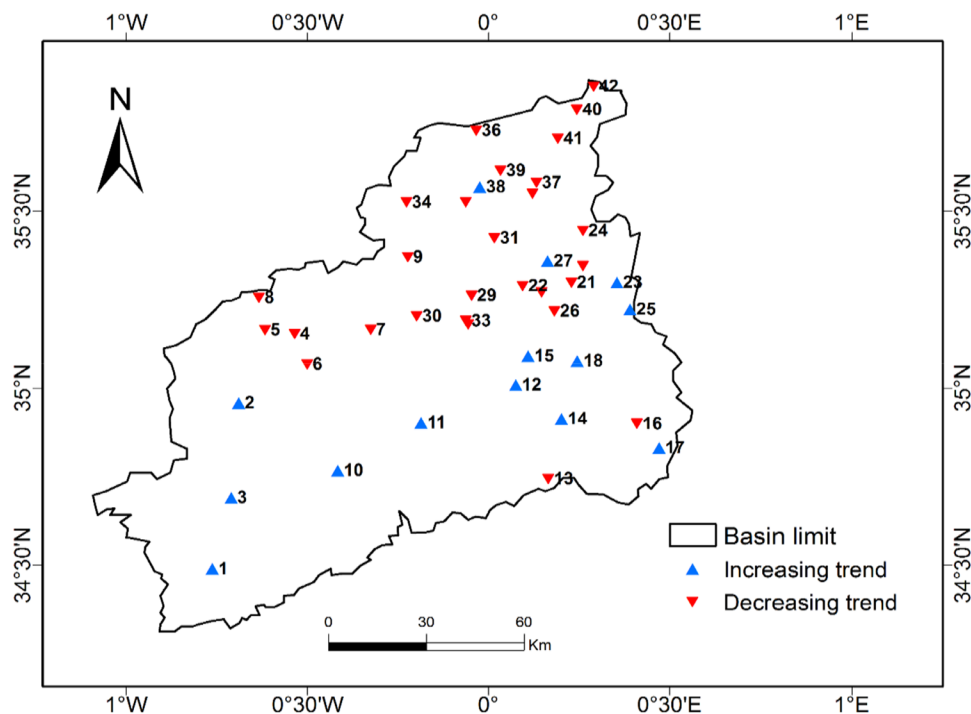
Spatial character of the frequency of drought occurrences

It is a natural phenomenon that the droughts vary based on time and space. The regional distribution of drought was interpolated and mapped using drought events with SPI values less than − 1.0 for 6- and 12-month timescales. Figure 10a shows the spatial distribution of relative frequency of drought (%) for 6-month SPI. From the figure, one can understand that the central and southwestern regions are characterized as drought areas comparatively often than the northeastern region.

Figure 10b shows the frequency drought map of 12-month SPI which infers that northern and western regions of the basin experienced frequent drought than southern and eastern parts of the basin. Figure 10a, b shows that there was an impact on the long-term water resources in both western and northern parts. In case of central-southwest region, there was an influence upon medium-term water supplies. The variation in the frequency values was found to be very low for two time scales while the frequency was higher in 12-month SPI compared to 6-month SPI in overall. In a previous study Vicente-Serrano et al. (2009), also found that the drought frequency changed according to the time scale in Spain.

At 12-month time steps, the northern and central parts of the basin experienced higher occurrence of severe droughts (Fig. 11a). The state of drought in this figure corresponds to SPI values between − 1.50 to − 1.99, i.e. severe drought conditions. Extreme drought occurrences (− 2 and less), on the other hand, are more pronounced in the eastern and southwestern parts of the basin (Fig. 11b). This means that

the eastern and southwestern parts suffer from extreme drought conditions frequently while the northwestern and central parts of the study area suffer from frequent severe drought conditions. In parallel to the observations made by Mellak and Souag-Gamane (2020), who assessed maximum drought severity in Northern Algeria using Copulas. Their results showed that the western part of the region is the most affected by severe droughts. On the other hand, Achour et al. (2020) assessed drought in the plains of northwestern Algeria using the standardized precipitation index during the period 1960–2010. The results indicate that the region affected by a severe drought, on the contrary, of the eastern part, where the drought duration and severity are decreased.

Conclusion

In this study, the spatial and temporal variations of rainfall as well as drought severity were analyzed for a total of 42-year-long time series in the Macta basin (northwest of Algeria). The Mann–Kendall (MK) test, Sen's slope test estimator, and Innovative Trend Analysis (ITA) method were used to determine the presence of either a positive or a negative trend in rainfall data with their statistical significance. The study also adopted the standardized precipitation index (SPI) to assess the spatial–temporal variations of meteorological drought over different time scales for the study period. The results achieved from MK test and ITA method inferred that the sub-region experienced decreasing trends in the northern part which is proximity to Mediterranean Sea coastal area in

Table 3 Mann–Kendall *Z* values (direction) and change percentage of seasonal and annual rainfall (1970–2011)

| No	Station code	Autumn		Winter		Spring		Summer		Annual	
		Z-value	% Change	Z-value	% Change	Z-value	% Change	Z-value	% Change	Z-value	% Change
1	110102	**2.15**	25.43	1.28	12.71	1.02	14.03	**2.32**	12.01	**3.16**	84.76
2	110201	**1.99**	18.27	0.00	− 0.06	− 0.08	− 2.00	− 0.27	− 0.48	0.55	13.61
3	110203	1.86	16.43	− 1.15	− 8.50	− 0.35	− 12.37	0.22	0.52	− 0.23	− 4.81
4	110304	0.75	5.43	− 1.60	− 14.70	− 1.13	− 19.70	0.00	0.00	− 1.58	− 32.29
5	110305	1.51	16.98	− 0.43	− 4.53	**− 2.06**	− 14.87	0.49	0.51	− 0.35	− 5.25
6	110309	0.46	5.07	0.74	8.89	− 1.11	− 24.62	− 0.73	− 0.87	− 1.08	− 26.21
7	110312	0.13	1.17	− 1.06	− 10.29	− 1.13	− 18.40	0.87	0.00	− 1.45	− 30.10
8	110314	− 0.21	− 3.92	− 1.34	− 14.15	− 1.47	− 26.50	− 1.28	− 1.04	**− 2.35**	− 51.19
9	110402	1.34	10.27	− 0.85	− 7.73	− 0.60	− 18.08	− 0.11	− 0.05	− 1.08	− 17.62
10	110501	**2.49**	21.63	− 0.08	− 0.61	− 0.44	− 8.54	0.86	2.54	1.13	15.87
11	110802	**3.62**	35.24	0.86	8.62	1.17	9.48	1.75	4.67	**2.86**	61.69
12	111102	1.94	17.46	− 0.04	− 0.90	− 0.52	− 5.62	− 0.02	0.00	0.65	12.00
13	111103	1.56	15.14	0.28	2.20	− 0.08	− 8.90	0.73	0.55	0.26	17.55
14	111112	**2.80**	27.89	0.55	5.44	0.53	− 1.66	1.17	1.63	1.47	42.54
15	111201	1.29	13.51	− 0.56	− 6.30	− 0.06	− 7.73	0.62	0.75	− 0.46	− 9.65
16	111204	1.00	9.74	− 1.20	− 12.93	− 1.73	− 14.78	0.71	1.71	− 0.26	− 3.89
17	111210	1.30	9.71	0.05	0.87	− 0.63	− 4.93	0.27	0.74	0.35	4.17
18	111217	**2.55**	25.11	1.27	19.71	1.02	7.81	1.08	1.34	1.85	62.25
19	111401	1.57	16.58	0.00	0.00	− 0.64	− 6.72	1.14	0.64	1.04	20.42
20	111402	**2.45**	19.52	− 0.07	− 0.34	− 0.40	− 4.31	1.67	1.41	0.82	13.07
21	111405	0.91	7.02	− 1.06	− 12.50	− 1.47	− 21.09	0.10	0.62	**− 2.02**	− 40.22
22	111413	1.70	13.73	0.24	13.78	− 1.34	− 9.21	− 0.55	0.00	− 0.48	− 7.90
23	111414	1.65	14.05	− 0.11	− 1.17	− 1.19	− 10.73	1.05	− 2.33	0.39	8.16
24	111417	**3.27**	23.34	1.93	21.22	0.74	1.05	1.11	1.05	**2.47**	55.29
25	111418	0.93	7.90	− 0.67	− 10.34	− 0.39	− 6.40	0.25	0.00	− 0.09	− 3.18
26	111424	− 0.57	− 4.03	− 1.60	− 19.02	− 0.66	− 4.49	− 0.62	− 0.72	− 1.58	− 32.10
27	111429	**2.40**	26.82	0.20	3.79	0.13	0.65	1.04	0.85	1.77	38.21
28	111502	1.29	12.31	0.31	3.36	− 0.95	− 15.96	− 0.40	0.00	0.09	1.68
29	111503	0.30	2.01	− 0.48	− 4.56	− 0.89	− 24.89	0.29	0.00	− 1.47	− 32.06
30	111508	0.50	4.92	− 1.24	− 7.86	− 1.18	− 24.71	− 0.75	− 0.99	**− 2.85**	− 36.24
31	111509	1.55	14.60	0.30	2.59	− 1.11	− 20.06	**2.24**	1.63	− 0.23	− 5.84
32	111511	1.56	12.12	− 0.62	− 6.60	− 0.91	− 21.64	0.22	0.00	− 0.81	− 19.07
33	111516	1.61	15.96	0.03	0.17	− 0.73	− 17.12	− 0.36	− 0.09	0.65	11.15
34	111604	1.17	10.86	− 0.27	− 2.61	**− 2.44**	− 23.37	− 0.75	0.00	− 0.66	− 11.81
35	111605	1.51	− 12.81	0.82	− 5.01	− 1.79	− 23.61	− 0.30	0.00	− 0.54	− 10.12
36	111606	0.81	6.00	0.03	0.24	− 1.52	− 23.37	− 1.19	− 0.85	− 1.46	− 27.10
37	111607	0.79	6.12	0.00	− 0.60	− 1.83	− 23.06	0.03	0.00	− 1.02	− 23.45
38	111610	**2.43**	28.92	1.82	24.99	1.27	11.99	**2.71**	2.99	**2.21**	74.42
39	111611	1.17	10.56	− 0.48	− 4.96	− 0.35	− 21.37	− 0.36	− 0.53	− 0.91	− 14.20
40	111612	1.11	10.88	0.17	1.04	0.04	0.75	0.67	0.00	− 0.33	− 4.77
41	111616	1.84	16.03	− 0.56	− 9.00	− 0.35	− 9.25	− 1.72	− 0.38	− 0.07	− 6.31
42	111617	1.42	13.62	− 1.21	− 11.60	− 1.76	− 14.72	− 0.72	0.00	− 1.52	− 24.27

Explanation: bold values indicate significant trend

the Macta basin. Further, it was also inferred that the southern trends were found to be increasing. According to the current study results, the ITA method exhibited few advantages in comparison with MK trend test. To be precise, the ITA method detailed the trends of annual total precipitation data with assessment of different values, such as low, medium and high. All the stations, according to the computed SPI values in both time scales, experienced peak intensities of
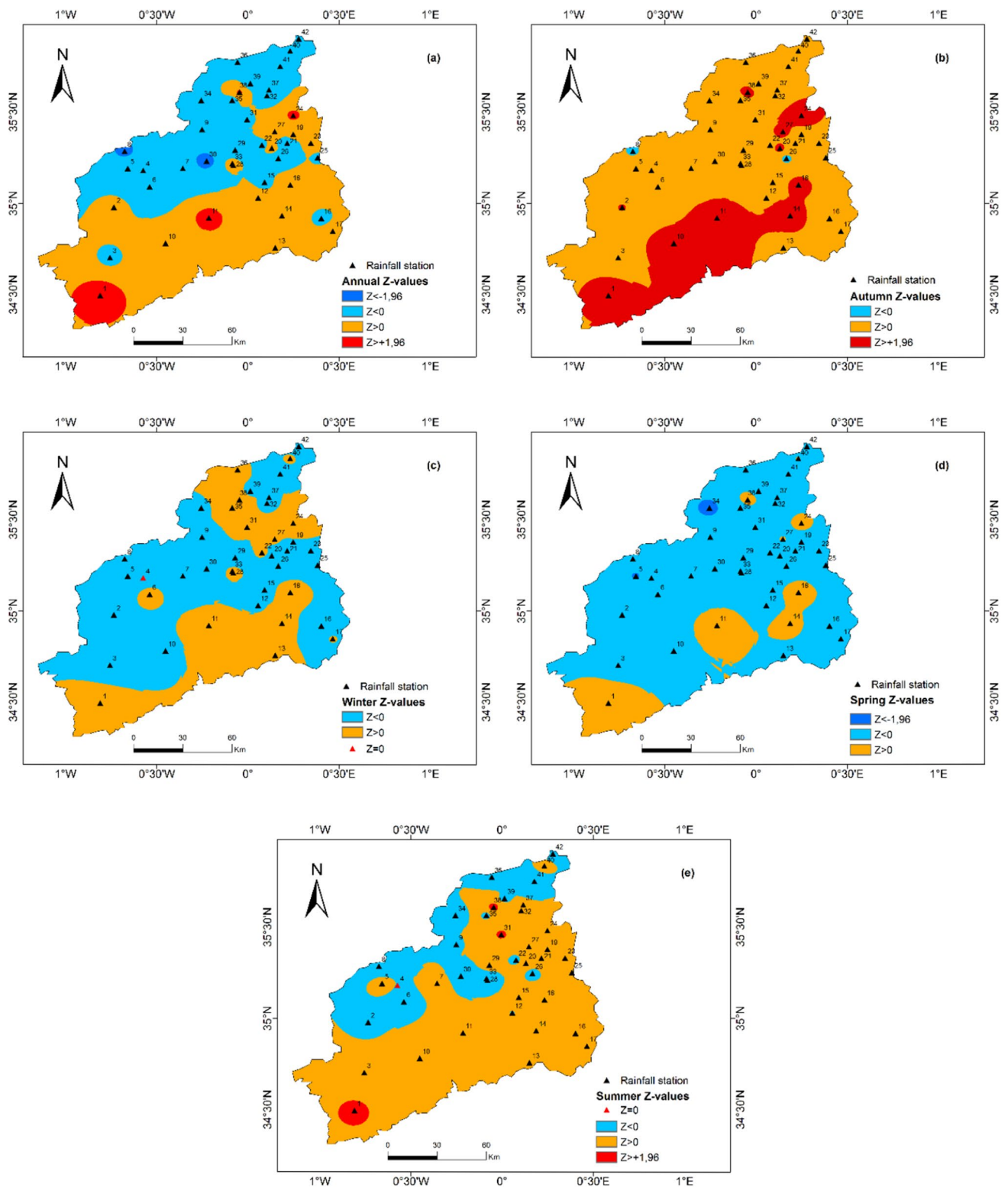
Fig 5 Spatial interpolation by Z-values of Mann–Kendall test for annual and seasonal rainfall trends. Values larger than 1.96 or lower than 1.96 indicate a significant trend (95% confidence level)
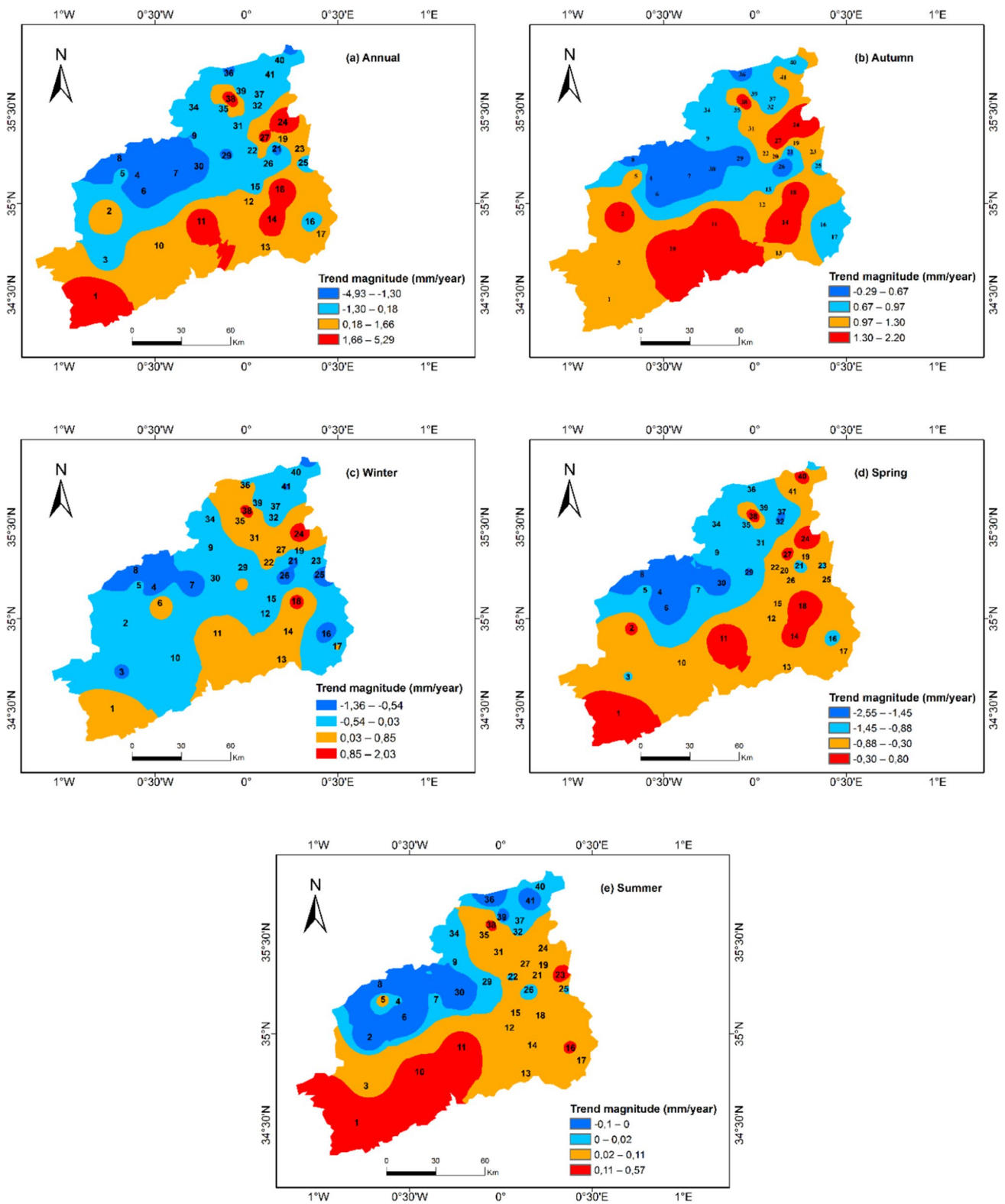
Fig 6 Spatial distribution patterns of trend magnitude for 42 selected rainfall stations at annual and seasonal time scales

**Table 4** Drought characteristics of 12-month time scale in the Macta basin

		Observed Peak intensity			Most intense duration (≤ − 2.0 for consecutive months)				Longest duration (≤ − 1.0 for consecutive months)				RF
No	Station code	SPI	Year	Month	D(mo)	Years	M	MI	D(mo)	Years	M	MI	(%)
1	110102	− 2.94	1978	Sep	7	77–78	− 18.81	− 2.69	34	76–79	− 70.22	− 2.07	13.10
2	110201	− 3.28	1979	May	11	1979	− 31.79	− 2.89	26	78–80	− 52.36	− 2.01	14.09
3	110203	− 3.28	1983	Dec	13	88–89	− 30.04	− 2.31	17	88–89	− 35.68	− 2.10	14.68
4	110304	− 2.43	1983	Dec	4	83–84	− 8.51	− 2.13	11	81–82	− 19.61	− 1.78	15.87
5	110305	− 3.16	1983	Dec	6	83–84	− 15.05	− 2.51	16	92–93	− 25.04	− 1.57	16.87
6	110309	− 3.29	1983	Dec	6	83–84	− 15.92	− 2.65	12	83–84	− 19.01	− 1.58	14.09
7	110312	− 3.13	1997	Jun	7	97–98	− 18.57	− 2.65	26	89–91	− 38.53	− 1.48	18.06
8	110314	− 3.08	1997	Jul	8	97–98	− 21.29	− 2.66	12	97–98	− 27.35	− 2.28	13.49
9	110402	− 2.52	1983	Dec	4	97–98	− 8.29	− 2.07	18	88–90	− 28.51	− 1.58	17.66
10	110501	− 3.17	1983	Dec	6	83–84	− 15.18	− 2.53	13	98–99	− 22.77	− 1.75	15.87
11	110802	− 3.59	1974	Sep	12	74–75	− 38.56	− 3.21	18	83–84	− 40.61	− 2.26	12.90
12	111102	− 3.43	1983	Dec	8	83–84	− 20.62	− 2.58	16	89–90	− 33.01	− 2.06	14.68
13	111103	− 3.59	1983	Dec	12	83–84	− 36.04	− 3.00	24	80–82	− 34.19	− 1.42	11.11
14	111112	− 3.03	1984	Jan	9	1989	− 21.46	− 2.38	33	88–90	− 58.31	− 1.77	13.49
15	111201	− 3.25	1978	Sep	11	83–84	− 27.54	− 2.50	16	77–79	− 36.05	− 2.25	12.10
16	111204	− 2.76	1983	Dec	6	2005	− 15.74	− 2.62	10	1993	− 19.87	− 1.99	14.09
17	111210	− 2.94	1983	Dec	4	83–84	− 10.35	− 2.59	19	83–84	− 30.65	− 1.61	12.90
18	111217	− 2.68	1983	Dec	6	1978	− 13.58	− 2.26	19	85–86	− 25.91	− 1.36	15.08
19	111401	− 2.32	1974	Jan	7	73–74	− 10.52	− 1.50	12	88–89	− 17.16	− 1.43	15.48
20	111402	− 3.06	1983	Dec	4	83–84	− 10.63	− 2.66	12	83–84	− 22.91	− 1.91	16.07
21	111405	− 2.71	1983	Dec	3	83–84	− 7.51	− 2.50	9	2000	− 16.02	− 1.78	16.47
22	111413	− 3.44	1983	Nov	10	81–82	− 22.18	− 2.22	12	89	− 18.61	− 1.55	15.87
23	111414	− 2.73	1983	Dec	3	83–84	− 7.03	− 2.34	10	80–81	− 13.41	− 1.34	15.87
24	111417	− 3.04	1982	Jan	10	81–82	− 24.57	− 2.46	19	81–82	− 37.76	− 1.99	12.50
25	111418	− 2.81	2000	May	8	2000	− 21.62	− 2.70	27	00–02	− 48.22	− 1.79	13.29
26	111424	− 2.27	2000	Mar	2	1982	− 4.16	− 2.08	10	2000	− 15.66	− 1.57	13.69
27	111429	− 3.01	1977	Apr	8	1977	− 20.38	− 2.55	21	76–77	− 38.71	− 1.84	17.06
28	111502	− 2.80	1982	Jan	5	81–82	− 11.76	− 2.35	12	83–84	− 19.55	− 1.63	18.45
29	111503	− 2.67	1983	Dec	5	83–84	− 11.36	− 2.27	11	81–82	− 16.71	− 1.52	13.69
30	111508	− 2.51	1983	Dec	4	1997	− 8.51	− 2.13	10	81–82	− 14.48	− 1.45	16.67
31	111509	− 3.93	1982	Mar	5	1982	− 11.71	− 2.34	10	81–82	− 22.15	− 2.22	16.27
32	111511	− 2.70	1982	Mar	8	1982	− 17.52	− 2.19	13	88–89	− 22.47	− 1.73	15.67
33	111516	− 2.50	1983	Dec	7	1982	− 16.71	− 2.39	12	81–82	− 26.58	− 2.22	14.88
34	111604	− 3.15	1983	Dec	6	1997	− 15.71	− 2.62	14	88–89	− 21.34	− 1.52	15.48
35	111605	− 2.12	1982	Dec	2	1982	− 4.37	− 2.19	22	80–82	− 40.31	− 1.83	16.47
36	111606	− 2.83	1982	Sep	6	81–82	− 16.43	− 2.74	15	01–03	− 28.44	− 1.90	18.65
37	111607	− 2.23	1999	Aug	4	1999	− 8.53	− 2.13	10	2000	− 13.26	− 1.33	16.47
38	111610	− 2.54	1982	Sep	9	1984	− 19.22	− 2.14	13	83–84	− 25.59	− 1.97	14.88
39	111611	− 2.72	1982	Apr	7	1982	− 17.91	− 2.56	14	88–89	− 26.23	− 1.87	14.48
40	111612	− 2.88	1983	Dec	5	1982	− 11.64	− 2.33	16	88–90	− 26.48	− 1.66	15.08
41	111616	− 2.51	1992	Nov	3	92–93	− 7.15	− 2.38	21	92–93	− 39.04	− 1.86	16.27
42	111617	− 2.49	1982	Sep	7	1982	− 16.31	− 2.33	14	94–95	− 24.57	− 1.76	14.68

D(mo) Duration (month), M Magnitude, MI Mean Intensity, RF Relative Frequency

less than − 2, thus it is segregated under extreme classification. Majority of the peak intensities occurred in the 1980s during winter season. The longest drought lasted for 34 months from April 1976 to January 1979 in the southwest region. The peak intensity of this drought was − 2.94, its magnitude was − 70.22, and its mean intensity was − 2.07.
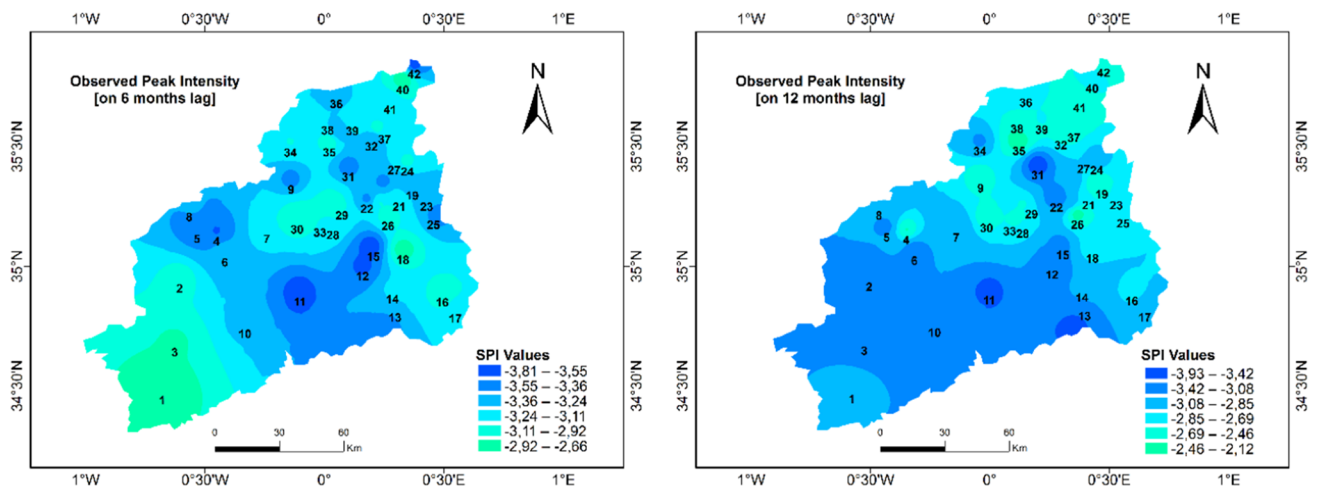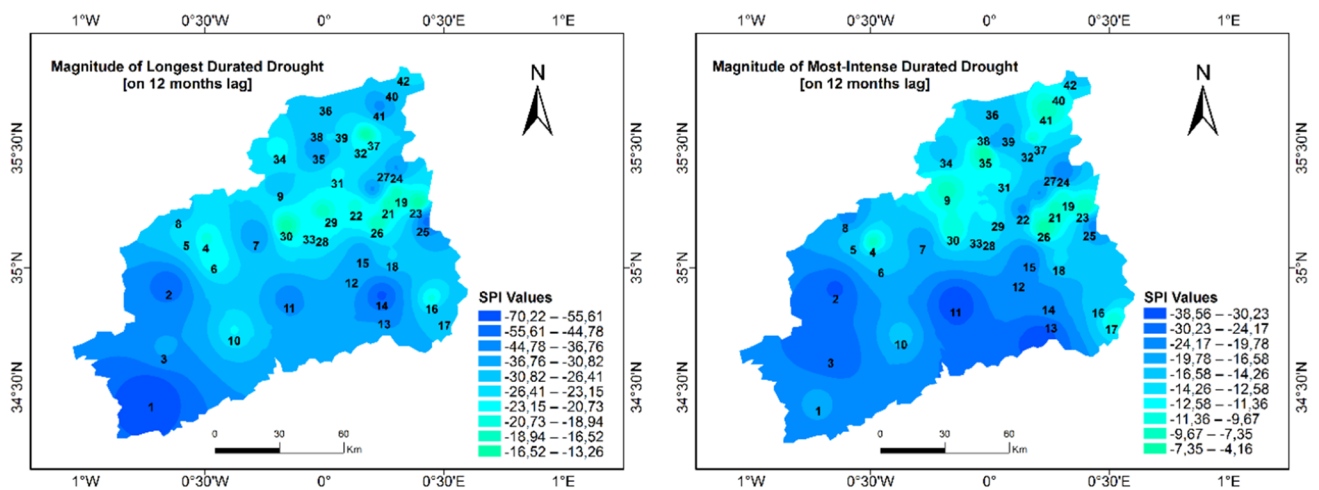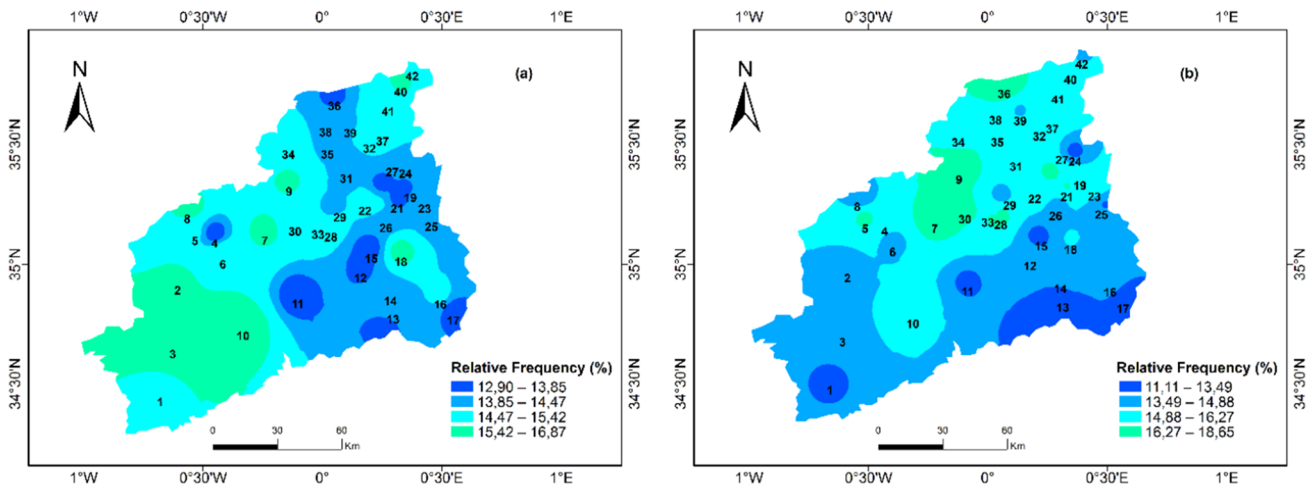
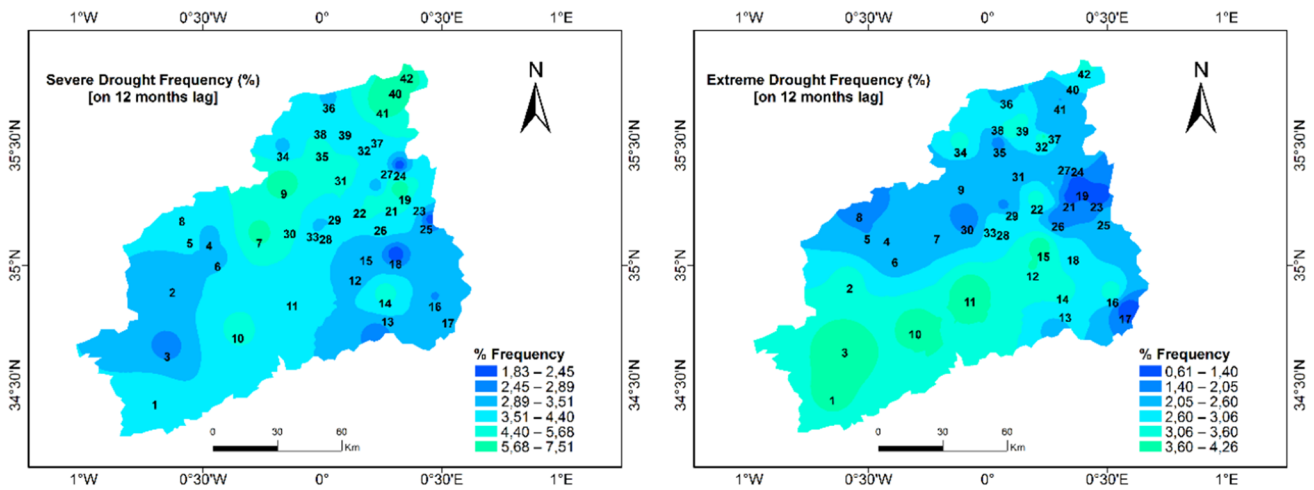**Fig 7** Observed peak intensity drought map at **a** 6-month and **b** 12-month time scale
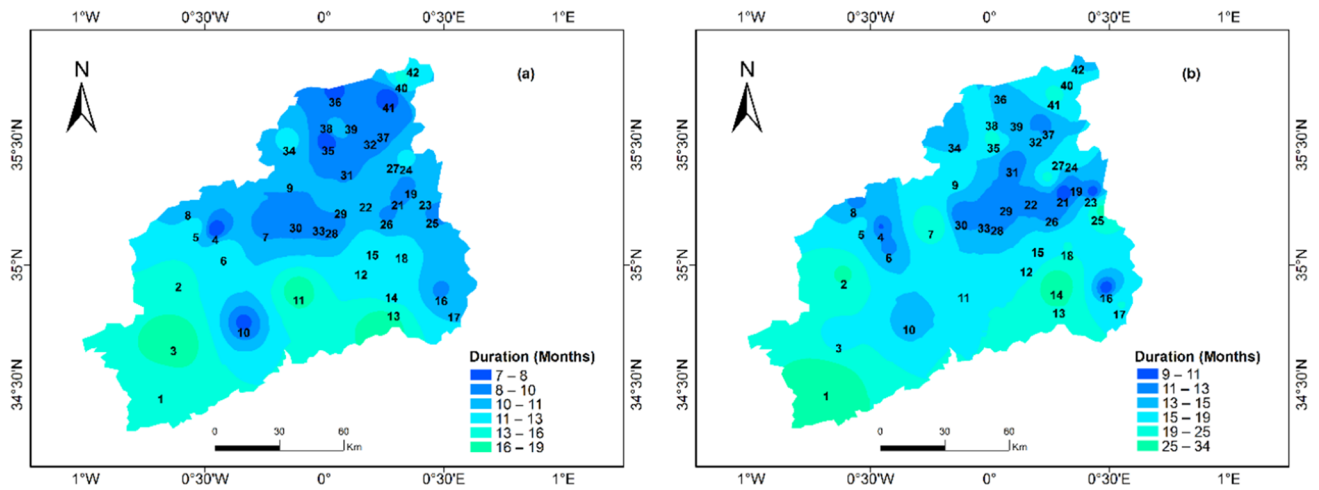
Fig 8 Longest duration droughts map at **a** 6-month and **b** 12-month time scale

Fig 9 Magnitude for **a** longest and **b** most-intense duration droughts on 12-month time step

Fig 10 Spatial distribution of relative frequency drought map at **a** 6-month and **b** 12-month time scale

Fig 11 Severe and extreme drought occurrences at 12-month time steps

The drought of 1997–1998, which occurred in the northwestern part with a duration of 12 months recorded a magnitude of − 27.35 and a mean intensity of − 2.28 and this had greatly impacted the study area. The spatial distribution of relative frequency of drought (%) for the 6-month SPI shows that the central and southwestern regions are characterized as drought areas more frequently than the northeastern region. Further, the long-term frequency drought shows that northern and western regions have experienced drought more frequently than the southern and eastern parts of the study area. This means that long-term water resources have been affected in the northern and western parts. In the central-southwest, however, medium-term water supplies have been influenced.

Finally, our findings show that severe drought conditions are more prevalent in the northern part of the basin than the other parts on a 12-month time scale. Drought

duration varies between 9 and 37 months, with an average of 20 months. Thus, this is a highly sensitive area that has high vulnerabilities towards droughts compared to other regions of the Macta basin. The primary reason behind continuous severe and extremely severe drought conditions might be lower-than-normal precipitation amounts. This would have been a result of immanent anticyclonic systems over the eastern part of the Mediterranean basin. Based on the past drought event observations, one can expect severe droughts frequently in the upcoming future. The national agency for hydraulic resources should take the current study results under consideration when implementing different strategies against droughts, for instance, knowledge transfer about conventional and unconventional resources into implementation, such as seawater desalination, wastewater recycling etc. These measures could positively meet the current and future water needs as the population is predicted to increase by

40–50% within 2030 (45–50 million). The water resources are highly important for agricultural and industrial activities which may undergo expansion and modernization.

Compliance with ethical standards

Conflict of interest On behalf of all authors, the corresponding author states that there is no conflict of interest.

References

Achite M, Buttafuoco G, Toubal KA, Luca F (2017) Precipitation spatial variability and dry areas temporal stability for different elevation classes in the Macta basin (Algeria). Environ Earth Sci 76(13):458. https://doi.org/10.1007/s12665-017-6794-3

Achour K, Meddi M, Zeroual A et al (2020) Spatio-temporal analysis and forecasting of drought in the plains of northwestern Algeria using the standardized precipitation index. J Earth Syst Sci 129:42. https://doi.org/10.1007/s12040-019-1306-3

Ahmad I, Zhang F, Tayyab M et al (2018) Spatiotemporal analysis of precipitation variability in annual, seasonal and extreme values over upper Indus River basin. Atmos Res 213:346–360. https://doi.org/10.1016/j.atmosres.2018.06.019

Alashan S (2018) An improved version of innovative trend analyses. Arab J Geosci 11(3):50–56. https://doi.org/10.1007/s12517-018-3393-x

Azam M, Park H, Maeng SJ, Kim HS (2017) Regionalization of drought across South Korea using multivariate methods. Water 10:24. https://doi.org/10.3390/w10010024

Azam M, Maeng S, Kim HS, Murtazaev A (2018) Copula-based stochastic simulation for regional drought risk assessment in South Korea. Water 10:359. https://doi.org/10.3390/w10040359

Báez JC, Enrique Salvo A, García-Soto C, Real R, Márquez AL, Flores-Moya A (2019) Effects of the North Atlantic Oscillation (NAO) and meteorological variables on the annual Alcarria honey production in Spain. J Apic Res 58:788–791. https://doi.org/10.1080/00218839.2019.1635424

Batisani N, Yarnal B (2010) Rainfall variability and trends in semi-arid Botswana: implications for climate change adaptation policy. Appl Geogr 30:483–489. https://doi.org/10.1016/j.apgeog.2009.10.007

Belarbi H, Touaibia B, Boumechra N, Amiar S, Baghli N (2017) Sécheresse et modification de la relation pluie–débit : cas du bassin versant de l'Oued Sebdou (Algérie Occidentale). Hydrol Sci J 62:124–136. https://doi.org/10.1080/02626667.2015.1112394

Benzater B, Elouissi A, Benaricha B, Habi M (2019) Spatio-temporal trends in daily maximum rainfall in northwestern Algeria (Macta watershed case, Algeria). Arab J Geosci 12:370. https://doi.org/10.1007/s12517-019-4488-8

Berhail S (2019) The impact of climate change on groundwater resources in northwestern Algeria. Arab J Geosci 12:770. https://doi.org/10.1007/s12517-019-4776-3

Bougara H, Hamed KB, Borgemeister C, Tischbein B, Kumar N (2020) Analyzing trend and variability of rainfall in the Tafna basin (Northwestern Algeria). Atmos 11:347. https://doi.org/10.3390/atmos11040347

Brunetti M, Maugeri M, Monti F, Nanni T (2004) Changes in daily precipitation frequency and distribution in Italy over the last 120 years. J Geophys Res Atmos 109:1–16 ((**D05102**))

Caloiero T, Coscarelli R, Ferrari E (2019) Assessment of seasonal and annual rainfall trend in Calabria (southern Italy) with the ITA method. J Hydroinf. https://doi.org/10.2166/hydro.2019.138

Chang J, Wei J, Wang Y, Yuan M, Guo J (2016) Precipitation and runoff variations in the Yellow River Basin of China. J Hydroinf 19:138–155. https://doi.org/10.2166/hydro.2016.047

Da Silva RM, Santos CAG, Moreira M, Corte-Real J, Silva VCL, Medeiros IC (2015) Rainfall and river flow trends using Mann–Kendall and Sen's slope estimator statistical tests in the Cobres River basin. Nat Hazards 77:1205–1221. https://doi.org/10.1007/s11069-015-1644-7

Dabanlı İ, Şen Z, Yeleğen M, Şişman E, Selek B, Güçlü Y (2016) Trend assessment by the innovative-Şen method. Water Resour Manag 30(14):5193–5203. https://doi.org/10.1007/s11269-016-1478-4

Derdous O, Bouamrane A, Mrad D (2020) Spatiotemporal analysis of meteorological drought in a Mediterranean dry land: case of the Cheliff basin–Algeria. Model Earth Syst Environ. https://doi.org/10.1007/s40808-020-00951-2

Donat MG et al (2014) Changes in extreme temperature and precipitation in the Arab region: long-term trends and variability related to ENSO and NAO. Int J Climatol 34:581–592. https://doi.org/10.1002/joc.3707

Duhan D, Pandey A (2013) Statistical analysis of long term spatial and temporal trends of precipitation during 1901–2002 at Madhya Pradesh, India. Atmos Res 122:136–149. https://doi.org/10.1016/j.atmosres.2012.10.010

Dünkeloh A, Jacobeit J (2003) Circulation dynamics of Mediterranean precipitation variability 1948–98. Int J Climatol 23:1843–1866. https://doi.org/10.1002/joc.973

El Mahi A, Meddi M, Bravard JP (2012) Analyse du transport solide en suspension dans le bassin versant de l'Oued El Hammam (Algérie du Nord)/Analysis of sediment transport in the Wadi el Hammam basin, northern Algeria. Hydrol Sci J 57:1642–1661. https://doi.org/10.1080/02626667.2012.717700

Elouissi A, Habi M, Benaricha B, Boualem SA (2017) Climate change impact on rainfall spatio-temporal variability (Macta watershed case, Algeria). Arab J Geosci 10(22):496. https://doi.org/10.1007/s12517-017-3264-x

Gedefaw M, Yan D, Wang H, Qin T, Girma A, Abiyu A, Batsuren D (2018) Innovative trend analysis of annual and seasonal rainfall variability in Amhara regional state. Ethiop Atmose 9:326. https://doi.org/10.3390/atmos9090326

Geremew GM, Mini S, Abegaz A (2020) Spatiotemporal variability and trends in rainfall extremes in Enebsie Sar Midir district, Northwest Ethiopia. Mod Earth Syst Environ 6(2):1177–1187. https://doi.org/10.1007/s40808-020-00749-2

Ghenim AN, Megnounif A, Seddini A, Terfous A (2010) Fluctuations hydropluviométriques du bassin-versant de l'oued Tafna a` Béni Bahdel (Nord-Ouest algérien). Sécheresse 21:115–120

Ghosh KG (2019) Spatial and temporal appraisal of drought jeopardy over the Gangetic West Bengal, eastern India. Geoenviron Dis 6(1):1. https://doi.org/10.1186/s40677-018-0117-1

Gidey E, Dikinya O, Sebego R, Segosebe E, Zenebe A (2018) Analysis of the long-term agricultural drought onset, cessation, duration, frequency, severity and spatial extent using Vegetation Health Index (VHI) in Raya and its environs, Northern Ethiopia. Environ Syst Res 7(1):13. https://doi.org/10.1186/s40068-018-0115-z

Gocic M, Trajkovic S (2013) Analysis of changes in meteorological variables using Mann–Kendall and Sen's slope estimator statistical tests in Serbia. Glob Planet Chang 100:172–182. https://doi.org/10.1016/j.gloplacha.2012.10.014

Gyamfi C, Amaning-Adjei K, Anornu GK et al (2019) Evolutional characteristics of hydro-meteorological drought studied using standardized indices and wavelet analysis. Model Earth Syst Environ 5:455–469. https://doi.org/10.1007/s40808-019-00569-z

Hamlet AF, Lettenmaier DP (2000) Long-range climate forecasting and its use for water management in the Pacific Northwest region of North America. J Hydroinf 2:163–182. https://doi.org/10.2166/hydro.2000.0015

Hayes M, Svoboda M, Wall N, Widhalm M (2011) The Lincoln declaration on drought indices: universal meteorological drought index recommended. Bull Am Meteorol Soc 92(4):485–488. https://doi.org/10.1175/2010BAMS3103.1

Hosseinizadeh A, SeyedKaboli H, Zareie H, Akhondali A, Farjad B (2015) Impact of climate change on the severity, duration, and frequency of drought in a semi-arid agricultural basin. Geoenviron Dis 2:23. https://doi.org/10.1186/s40677-015-0031-8

Intergovernmental Panel on Climate Change (IPCC) (2013) Climate change 2013: the physical science basis. In: Stocker TF, Qin D, Plattner G-K, Tignor M, Allen SK, Boschung J, Nauels A, Xia Y, Bex V, Midgley PM (eds) Contribution of working group I to the fifth assessment report of the intergovernmental panel on climate change. Cambridge University Press, Cambridge, p 1535

Jemai H, Ellouze M, Abida H, Laignel B (2018) Spatial and temporal variability of rainfall: case of Bizerte-Ichkeul Basin (Northern Tunisia). Arab J Geosci 11(8):177. https://doi.org/10.1007/s12517-018-3482-x

Ji L, Peters A (2003) Assessing vegetation response to drought in the northern Great Plains using vegetation and drought indices. Remote Sens Environ 87(1):85–98. https://doi.org/10.1016/S0034-4257(03)00174-3

Kebede A, Raju UJP, Korecha D, Nigussie M (2020) Developing new drought indices with and without climate signal information over the Upper Blue Nile. Model Earth Syst Environ 6:151–161. https://doi.org/10.1007/s40808-019-00667-y

Kendall MG (1975) Rank correlation methods, 4th edn. Charles Griffin, London

Keyantash JA, Dracup JA (2002) The quantification of drought: an evaluation of drought indices. Bull Am Meteor Soc 83:1167–1180. https://doi.org/10.1175/1520-0477-83.8.1167

Khalil A, Ullah S, Khan S, Manzoor S, Gul A, Shafiq M (2017) Applying time series and a non-parametric approach to predict pattern, variability, and number of rainy days per month. Pol J Environ Stud 26:635–642. https://doi.org/10.15244/pjoes/65155

Khedimallah A, Meddi M, Mahé G (2020) Characterization of the interannual variability of precipitation and runoff in the Cheliff and Medjerda basins (Algeria). J Earth Syst Sci 129:134. https://doi.org/10.1007/s12040-020-01385-1

Kim HS, Muhammad A, Maeng SJ (2016) Hydrologic modeling for simulation of rainfall-runoff at major control points of geum river watershed. Procedia Eng 154:504–512. https://doi.org/10.1016/j.proeng.2016.07.545

Knippertz P, Ulbrich U, Marques F, Corte-Real J (2003) Decadal changes in the link between El Niño and springtime North Atlantic oscillation and European-North African rainfall. Int J Climatol 23:1293–1311. https://doi.org/10.1002/joc.944

Krishnakumar KN, Prasada Rao GSLHV, Gopakumar CS (2009) Rainfall trends in twentieth century over Kerala, India. Atmos Environ 43:1940–1944. https://doi.org/10.1016/j.atmosenv.2008.12.053

Kumar M, Denis D, Suryavanshi S (2016) Long-term climatic trend analysis of Giridih district, Jharkhand (India) using statistical approach. Model Earth Syst Environ 2:116. https://doi.org/10.1007/s40808-016-0162-2

Laborde JP (1993) Cartes pluviométriques de l'Algérie du Nord a` l'échelle du 1/500 000, notice explicative. Agence Nationale des Ressources Hydrauliques, projet PNUD/ALG/88/021

Li YJ, Zheng XD, Lu F, Jing MA (2012) Analysis of drought evolvement characteristics based on standardized precipitation index in the Huaihe River basin. Procedia Eng 28:434–437. https://doi.org/10.1016/j.proeng.2012.01.746

Longobardi A, Villani P (2010) Trend analysis of annual and seasonal rainfall time series in the Mediterranean area. Int J Climatol 30:1538–1546. https://doi.org/10.1002/joc.2001

Machiwal D, Jha MK (2008) Comparative evaluation of statistical tests for time series analysis: application to hydrological time series. Hydrol Sci J 53:353–366. https://doi.org/10.1623/hysj.53.2.353

Maeng SJ, Azam M, Kim HS, Hwang JH (2017) Analysis of changes in spatio-temporal patterns of drought across South Korea. Water 9:679. https://doi.org/10.3390/w9090679

Mann HB (1945) Nonparametric tests against trend. Econometrica 13:245–259

Masih I, Maskey S, Mussá F, Trambauer P (2014) A review of droughts on the African continent: a geospatial and long-term perspective. Hydrol Earth Syst Sci 18(9):3635–3649. https://doi.org/10.5194/hess-18-3635-2014

McKee TB, Doesken NJ, Kleist J (1993) The relationship of drought frequency and duration to time scales. Proc Conf Appl Climatol 17(22):179–183

Meddi M, Talia A, Martin C (2009) Évolution récente des conditions climatiques et des écoulements sur le bassin versant de la Macta (Nord-Ouest de l'Algérie). Physio-Géo 3:61–84. https://doi.org/10.4000/physio-geo.686

Meddi M, Arkamose AA, Meddi H (2010a) Temporal variability of annual rainfall in the Macta and Tafna catchments, northwestern Algeria. Water Resour Manag 24(14):3817–3833. https://doi.org/10.1007/s11269-010-9635-7

Meddi M, Assani A, Meddi H (2010b) Temporal variability of annual rainfall in the Macta and Tafna catchments, Northwestern Algeria. Water Resour Manag 24:3817–3833. https://doi.org/10.1007/s11269-010-9635-7

Mekonen AA, Berlie AB, Ferede MB (2020) Spatial and temporal drought incidence analysis in the northeastern highlands of Ethiopia. Geoenviron Dis 7:10. https://doi.org/10.1186/s40677-020-0146-4

Mellak S, Souag-Gamane D (2020) Spatio-temporal analysis of maximum drought severity using Copulas in Northern Algeria. J Water Clim Chang. https://doi.org/10.2166/wcc.2020.070

Mishra AK, Singh VP (2010) A review of drought concepts. J Hydrol 391:202–216. https://doi.org/10.1016/j.jhydrol.2010.07.012

Nair SC, Mirajkar AB (2020) Spatio–temporal rainfall trend anomalies in Vidarbha region using historic and predicted data: a case study. Model Earth Syst Environ. https://doi.org/10.1007/s40808-020-00928-1

Nouaceur Z, Murarescu O (2016) Rainfall variability and trend analysis of annual rainfall in North Africa. Int J Atmospheric Sci 2016:1–12. https://doi.org/10.1155/2016/7230450

Oladipo EO (1985) A comparative performance analysis of three meteorological drought indices. Int J Climatol 5:655–664. https://doi.org/10.1002/joc.3370050607

Ouatiki H, Boudhar A, Ouhinou A et al (2019) Trend analysis of rainfall and drought over the Oum Er-Rbia River Basin in Morocco during 1970–2010. Arab J Geosci 12(4):128. https://doi.org/10.1007/s12517-019-4300-9

Pathak AA, Dodamani BM (2020) Trend analysis of rainfall, rainy days and drought: a case study of Ghataprabha River Basin, India. Model Earth Syst Environ 6:1–16. https://doi.org/10.1007/s40808-020-00798-7

Perrodon A (1957) Etude géologique des bassins néogènes sublittoraux de l'Algérie nord-occidentale. Bulletin du Service de la Carte géologique de l'Algérie 12:343–448

Potop V, Boroneant C, Mozny M, Stepanek P, Skalak P (2014) Observed spatiotemporal characteristics of drought on various time scales over the Czech Republic. Theor Appl Climatol 115:563–581. https://doi.org/10.1007/s00704-013-0908-y

Raghavan SV, Tue VM, Shie-Yui L (2013) Impact of climate change on future stream flow in the Dakbla river basin. J Hydroinf 16:231–244. https://doi.org/10.2166/hydro.2013.165

Rousta I, Olafsson H, Moniruzzaman M et al (2020) The 2000–2017 drought risk assessment of the western and southwestern basins

in Iran. Model Earth Syst Environ 6:1201–1221. https://doi.org/10.1007/s40808-020-00751-8

Şen PK (1968) Estimates of the regression coefficient based on Kendall's Tau. J Am Stat Assoc 63:1379–1389

Şen Z (2012) Innovative trend analysis methodology. J Hydrol Eng 17:1042–1046. https://doi.org/10.1061/(ASCE)HE.1943-5584.0000556

Şen Z (2014) Trend identification simulation and application. J Hydrol Eng 19:635–642. https://doi.org/10.1061/(ASCE)HE.1943-5584.0000811

Sen Z (2015) Innovative trend significance test and applications. Theor Appl Climatol 127:939–947. https://doi.org/10.1007/s00704-015-1681-x

Serencam U (2019) Innovative trend analysis of total annual rainfall and temperature variability case study: Yesilirmak region. Turkey Arab J Geosci 12:704. https://doi.org/10.1007/s12517-019-4903-1

Shifteh Somee B, Ezani A, Tabari H (2012) Spatiotemporal trends and change point of precipitation in Iran. Atmos Res 113:1–12. https://doi.org/10.1016/j.atmosres.2012.04.016

Sobhani B, Zengir VS (2020) Modeling, monitoring and forecasting of drought in south and southwestern Iran. Model Earth Syst Environ 6:63–71. https://doi.org/10.1007/s40808-019-00655-2

Sonmez FK, Komuscu AU, Erkan A, Turgu E (2005) An analysis of spatial and temporal dimension of drought vulnerability in Turkey using the standardized precipitation index. Nat Hazards 35(2):243–264. https://doi.org/10.1007/s11069-004-5704-7

Spinoni J, Naumann G, Carrao H, Barbosa P, Vogt J (2014) World drought frequency, duration, and severity for 1951–2010. Int J Climatol 34(8):2792–2804. https://doi.org/10.1002/joc.3875

Sultan B, Guan K, Kouressy M et al (2014) Robust features of future climate change impacts on sorghum yields in West Africa. Environ Res Lett 9:104006. https://doi.org/10.1088/1748-9326/9/10/104006

Theil H (1950) A rank invariant method of linear and polynomial regression analysis, part 3. Nederl Akad Wetensch Proc 53:1397–1412

Thompson SA (1999) Hydrology for water management. CRC Press, London, pp 286–317

Touchan R, Anchukaitis KJ, Meko DM et al (2011) Spatiotemporal drought variability in northwestern Africa over the last nine centuries. Clim Dyn 37(1):237–252. https://doi.org/10.1007/s00382-010-0804-4

Tramblay Y, Badi W, Driouech F, El Adlouni S, Neppel L, Servat E (2012) Climate change impacts on extreme precipitation in Morocco. Glob Planet Chang 82–83:104–114. https://doi.org/10.1016/j.gloplacha.2011.12.002

Vicente-Serrano SM, Beguería S, López-Moreno JI (2009) A Multiscalar drought index sensitive to global warming: the standardized precipitation evapotranspiration index. J Clim 23(7):1696–1718. https://doi.org/10.1175/2009JCLI2909.1

Wang L, Chen W, Zhou W, Chan JCL, Barriopedro D, Huang R (2010) Effect of the climate shift around mid 1970s on the relationship between wintertime Ural blocking circulation and East Asian climate. Int J Climatol 30:153–158. https://doi.org/10.1002/joc.1876

Wang Q, Wu J, Lei T et al (2014) Temporal-spatial characteristics of severe drought events and their impact on agriculture on a global scale. Quatern Int 349:10–21. https://doi.org/10.1016/j.quaint.2014.06.021

Wei W, Watkins DW (2011) Probabilistic streamflow forecasts based on hydrologic persistence and large-scale climate signals in central Texas. J Hydroinf 13:760–774. https://doi.org/10.2166/hydro.2010.133

WMO (2012) Standardized Precipitation Index User Guide. Svoboda M, Hayes M, Wood D (Eds.). (WMO-No. 1090), Geneva

Xu K, Milliman JD, Xu H (2010) Temporal trend of precipitation and runoff in major Chinese Rivers since 1951. Glob Planet Change 73:219–223. https://doi.org/10.1016/j.gloplacha.2010.07.002

Yue S, Hashino M (2003) Long term trends of annual and monthly precipitation in Japan. J Am Water Resour Assoc 39:587–596. https://doi.org/10.1111/j.1752-1688.2003.tb03677.x

Zargar A, Sadiq R, Naser B, Khan FI (2011) A review of drought indices. Environ Rev 19:333–349. https://doi.org/10.1139/a11-013

Zhang C, Zhu X, Fu G, Zhou H, Wang H (2014) The impacts of climate change on water diversion strategies for a water deficit reservoir. J Hydroinf 16:872–889. https://doi.org/10.2166/hydro.2013.053